AAS 17-704

DISTRIBUTED SPACECRAFT PATH PLANNING AND COLLISION AVOIDANCE VIA RECIPROCAL VELOCITY OBSTACLE APPROACH

Sittiporn Channumsin,[*] Gianmarco Radice,[†] and Matteo Ceriotti[‡]

This paper presents the development of a combines linear quadratic regulation and reciprocal velocity obstacle (LQR/RVO) control algorithm for multiple satellites during close proximity operations. The linear quadratic regulator (LQR) control effort drives the spacecraft towards their target position while the reciprocal velocity obstacle (RVO) provides collision avoidance capabilities. Each spacecraft maneuvers independently, without explicit communication or knowledge in term of collision avoidance decision making of the other spacecraft in the formation. To assess the performance of this novel controller different test cases are implemented. Numerical results show that this method guarantees safe and collision-free maneuvers for all the satellites in the formation and the control performance is presented in term of Δv and fuel consumption.

INTRODUCTION

Spacecraft formation flying (FF) can provide new and innovative ways of collecting scientific and observation data, enhance exploration capabilities and share this information between in-orbit systems and the ground. Small satellites are naturally suitable for this type of mission in which a large number of orbiting platforms can act as distributed instruments, thus exploiting the inherent redundancy, reconfiguration ability in the event of single point failures and enhanced mission capabilities offered by this approach including opportunities for cost reduction. One of the main challenges for these types of missions is however the reliable and robust control of the spacecraft maneuvers such as formation keeping or reconfiguration and critically, collision avoidance.

In order to avoid collisions real-time path planning in a dynamically changing environment is a key challenge that has been widely investigated for many years[1-8]. Close formation flying presents difficult control challenges as the number of elements in the formation increases or when proximity operations are required due to complex maneuvers with minimal fuel consumption and reliable collision avoidance systems. In addition, trajectory planning algorithms should be used to compute the initial plans of the mission and reactive methods should compute solutions in real time whenever a potential collision is detected. Moreover, a good scalability of the methods used is essential.

[*] Researcher, Geo-Informatics and Space Technology Development Agency (public organization), Bangkok 10210, Thailand. sittiporn@gistda.or.th.

[†] Professor, Singapore Institute of Technology, 138682, Singapore, Gianmarco.radice@singaporetech.edu.sg.

[‡] Lecturer in Space System Engineering, School of Engineering, Glasgow, G128QQ, United Kingdom. matteo.ceriotti@glasgow.ac.uk.

To account for these, the reciprocal velocity obstacle (RVO) developed by Berg[9] for marine vessels, is applied here. This approach takes inspiration from the velocity obstacle (VO)[10] that defines the set of all velocities that will result in a collision between two spacecraft at some point in time; selecting a velocity that lies outside the velocity obstacle ensures that no collision will occur. When many agents implementing the same navigation technique, share the same space, velocity obstacle methods may lead to undesirable behaviors such as oscillations or excessive deviations from the optimal trajectories. Several methods have been proposed to improve the implicit coordination among the agents. For instance, an agent may take only half of the responsibility to avoid an on-course collision, assuming that the other agents will do the same.

The RVO overcomes the intrinsic problem of oscillations present in the VO approach by selecting a new velocity that is the average between the current spacecraft velocity and a velocity that lies outside the other agent's velocity obstacle, then the motion of both will be free of collisions and oscillations. One of the advantages of this technique is that each agent does not take into account the decision-making plan to avoid collision of other agents. This is a key aspect for real time collision avoidance in a dynamic environment. RVO has been implemented in various application domains such as mobile roboticst[11, 12], UAV[13] and video games[14]

Following a brief definition of the relative motion dynamics[15] the design of the mixed LQR/RVO controller for path planning and collision avoidance for autonomous formation flying is presented in detail. Test cases and numerical simulations are then discussed and critically analysed before conclusions and future work are provided in the last section of this paper.

RELATIVE MOTION DYNAMICS

The formation flying spacecraft, assumed as a rigid body, is orbiting in the Earth Centered Inertial (ECI) coordinate system (X, Y, Z) as shown in Figure 1.

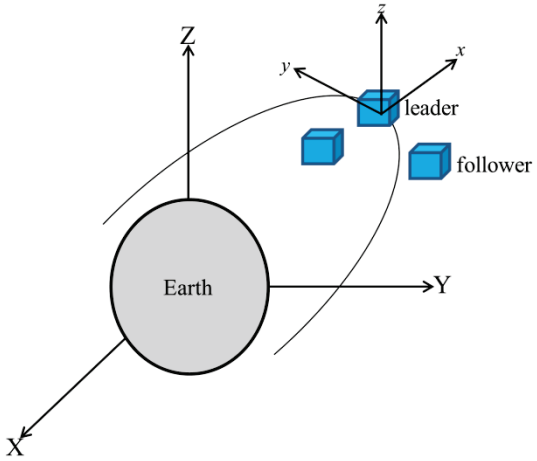

Figure 1. Relative orbit reference system.

The Local Vertical-Local Horizontal (LVLH) frame of reference is used to describe the relative motion dynamics (x (radial), y (along-track), z (cross-track)). The linearized relative dynamics[15] of the i^{th} follower with respect to the leader can be represented as:

$$\ddot{x}_i - 2\dot{\theta}\dot{y}_i - \ddot{\theta}y_i - \dot{\theta}^2 x_i = 2n^2\left(\frac{1+e\cos\theta}{1-e^2}\right)^3 x_i \tag{1}$$

$$\ddot{y}_i + 2\dot{\theta}\dot{x}_i + \ddot{\theta}x_i - \dot{\theta}^2 y_i = -n^2\left(\frac{1+e\cos\theta}{1-e^2}\right)^3 y_i \tag{2}$$

$$\ddot{z}_i = -n^2\left(\frac{1+e\cos\theta}{1-e^2}\right)^3 z_i \tag{3}$$

where n and e are the natural frequency and eccentricity of the reference orbit and θ is the true anomaly. $\dot{\theta}$ and $\ddot{\theta}$ are the angular velocity and acceleration of the reference orbit of leader spacecraft and defined as:

$$\dot{\theta} = \frac{n(1+e\cos\theta)^2}{(1-e^2)^{3/2}} \tag{4}$$

$$\ddot{\theta} = -\frac{2en\sin\theta\dot{\theta}}{(1-e^2)^{3/2}}(1+e\cos\theta) \tag{5}$$

To consider the control of the relative motion, Eqs. (1) – (3) can be transformed in a linear time-varying (LTV) system of equations in state-space $\boldsymbol{s}(t) = \begin{bmatrix} x & y & z & \dot{x} & \dot{y} & \dot{z} \end{bmatrix}^T$:

$$\dot{\boldsymbol{s}}(t) = \boldsymbol{A}(t)\boldsymbol{s}(t) + \boldsymbol{B}(t)\boldsymbol{u}(t) \tag{6}$$

where $\boldsymbol{u}(t)$ is control input, $\boldsymbol{A}(t)$ (relative dynamics matrix) and $\boldsymbol{B}(t)$ (control matrix) are defined as:

$$\boldsymbol{A}(t) = \begin{bmatrix} \mathbf{0}_3 & \boldsymbol{I}_3 \\ \boldsymbol{M}(t) & \boldsymbol{N}(t) \end{bmatrix} \quad \boldsymbol{B}(t) = \begin{bmatrix} \mathbf{0}_3 \\ \boldsymbol{I}_3 \end{bmatrix} \tag{7}$$

where $\mathbf{0}_3 \in \mathbb{R}^{3\times3}$, $\mathbf{I}_3 \in \mathbb{R}^{3\times3}$, $\boldsymbol{N}(t) = \begin{bmatrix} 0 & \dot{\theta} & 0 \\ -\dot{\theta} & 0 & 0 \\ 0 & 0 & 0 \end{bmatrix}$, $\boldsymbol{M}(t) = \begin{bmatrix} m_{11} & \ddot{\theta} & 0 \\ -\ddot{\theta} & m_{22} & 0 \\ 0 & 0 & m_{33} \end{bmatrix}$ and the matrix elements are given as:

$$\begin{aligned} m_{11} &= \dot{\theta}^2 + 2n^2\left(\frac{1+e\cos\theta}{1-e^2}\right)^3 \\ m_{22} &= \dot{\theta}^2 - n^2\left(\frac{1+e\cos\theta}{1-e^2}\right)^3 \\ m_{33} &= n^2\left(\frac{1+e\cos\theta}{1-e^2}\right)^3 \end{aligned} \tag{8}$$

The main perturbations to spacecraft in low Earth orbits are due to Earth oblateness (J_2) and atmospheric drag, particularly over long periods[16]. In this preliminary study, we ignore both effects.

LINEAR QUADRATIC REGULATION

In this paper, the LQR algorithm serves as the principal convergence driver during close proximity operations while RVO will ensure collision free maneuver including optimize fuel consumption. The multiple spacecraft LQR algorithm uses the linearized state dynamics from Eq. (6). To give a qualitative measure of system performance, a cost function J is introduced. By minimizing this cost function, the system can be brought from an initial state at t_0 to a final state at t_f with acceptable levels of state error and using acceptable and minimized levels of

control. A common choice for the performance index is to use a quadratic form of the terminal state and an integral of the quadratic form of the current state and control. The general form of the LQR cost function is defined as:

$$J = \frac{1}{2}\int_{t_0}^{t_f} \left(\boldsymbol{s}(t)^T \boldsymbol{Q}(t)\boldsymbol{s}(t) + \boldsymbol{u}(t)^T \boldsymbol{R}(t)\boldsymbol{u}(t) \right) dt \tag{9}$$

where $\boldsymbol{Q}(t)$ is the state gain matrix, $\boldsymbol{R}(t)$ is the control effort gain matrix. The optimal feedback control is given by:

$$\boldsymbol{u(t)} = -\boldsymbol{R}^{-1}(t)\left(\boldsymbol{B}^T(t)\boldsymbol{G}(t) \right)\boldsymbol{s}(t) = -\boldsymbol{K}_{LQR}\boldsymbol{s}(t) \tag{10}$$

where $\boldsymbol{K}_{LQR}$ is the optimal state feedback and $\boldsymbol{G}(t)$ is the solution of the algebraic Riccati equation.

VELOCITY OBSTACLE

Let us assume two spacecraft with radius r_A and radius r_B at position and velocities (p_A and p_B) with velocities (v_A and v_B) as shown in Figure 2. The velocity obstacle (VO) for agent A induced by a moving obstacle B is created as follows. We first determine the collision cone (CC) of agent A by extending the radius of agent B as a disc: $D(p_B, r_A + r_B)$ centered on p_B with radius $r_A + r_B$. $v_{A,B}$ is the relative velocity of A with respect to B and $\lambda_{A,B}$ is a direction of $v_{A,B}$. Any relative velocity $v_{A,B}$ that lies in $CC_{A|B}$ will lead to a collision.

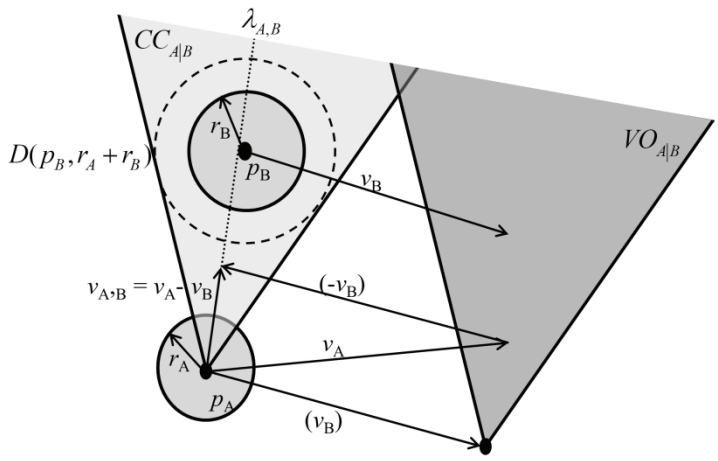

Figure 2. Velocity obstacle for agent A induced by obstacle B.

A set of relative CC for a agent A induced by a moving obstacle B ($CC_{A|B}$) is formally defined as:

$$CC_{A|B} = \left\{ v_{A,B} \,\middle|\, \lambda_{A,B} \cap D(p_B, r_A + r_B) \neq \varnothing \right\} \tag{11}$$

In multi agent scenarios, the agent will have to deal with multiple moving obstacles hence it is more convenient to create a set of absolute velocities of the agent. Formally, the velocity obstacle for an agent A induced by agent B is defined as:

$$VO_{A|B} = CC_{A|B} \oplus v_B \tag{12}$$

where $\oplus$ is the Minkowski sum of two sets of vectors A and B $A \oplus B = \{a+b | a \in A, b \in B\}$.

In case of multiple agents,agent A can create all velocity obstacles for all agents in the environment. The resulting set of velocity obstacle is generated by a union of all computed obstacles:

$$VO_A = \bigcup_{i=1}^{m} VO_{A|B_i} \tag{13}$$

Unfortunately, the velocity obstacle approach does not work very well for local collision avoidance within a group of virtual agents where each virtual agent is actively changing its velocity to avoid the other virtual agents, since it assumes that other virtual agents may not change their velocities. If all virtual agents were to use velocity obstacles to choose a new velocity, there would be oscillations in the motion of the virtual agents between successive time steps[9].

RECIPROCAL VELOCITY OBSTACLE (RVO)

To overcome the problem of oscillations, the reciprocal velocity obstacle (RVO) was introduced by Berg et al[9]. The surrounding moving obstacles are in fact also proactive agents and thus aim to avoid collisions. RVO for each agent takes care of half of the collision avoidance and the apex of the VO can be translated to $(v_A + v_B)/2$ instead of v_B as shown in Figure 3.

The reciprocal velocity obstacle[9] for agent A induced by agent B is thus defined as:

$$RVO_{A|B} = \left\{ v \middle| 2v - v_A \in VO_{A|B} \right\} \tag{14}$$

This leads to the property that if every agent chooses an optimal velocity (v_A^{opt}) outside of the RVO closest to the preferred velocity (v_A^{pref}), the agent will pass on the same side. However, each agent optimizes its commanded velocity with respect to a preferred velocity in order to make progress towards its goal location. This can lead to reciprocal motion, i.e. both agents first try to avoid towards the same side and then to the other side. In a situation with perfect symmetry and sensing, this behavior would continue indefinitely.

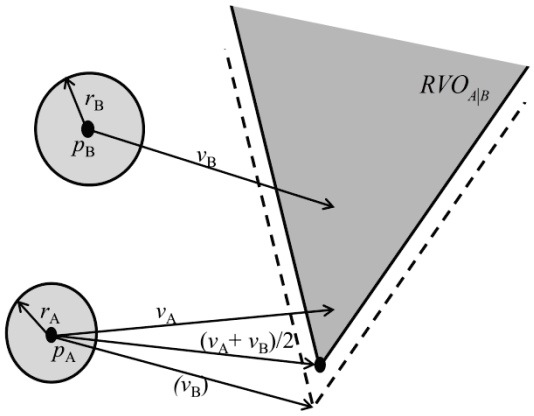

Figure 3. Reciprocal velocity obstacle for agent A induced by obstacle B.

CLEARPATH

A method to efficiently select collision free velocity is through ClearPath algorithm developed by Guy et al[17]. ClearPath follows the general idea that the collision-free velocity (v_A^{opt}) is closest to v_A^{pref} . Figure 4, shows the interpretation of the algorithm. The projection of v_A^{pref} is onto each reciprocal velocity obstacle. All points that are within another obstacle are discarded and from the remaining set the one closest to v_A^{pref} is selected. v_A^{opt} is determined as the desired velocity for LQR control to calculate the control input (***u(t)***).

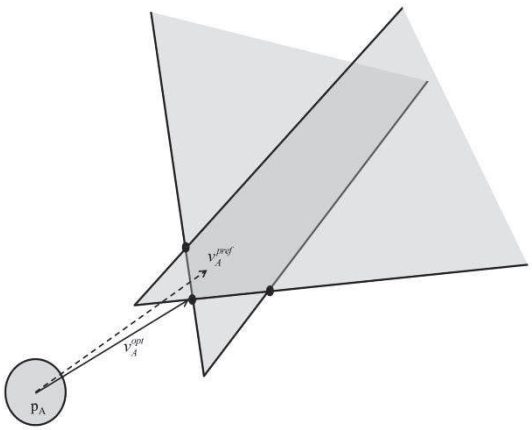

Figure 4. ClearPath enumerates intersection points for all pairs of RVO and projection points. The point closest to the preferred velocity (dash line) and outside of all RVOs is selected as the new velocity (solid line).

In summary, the LQR/RVO algorithms are implemented as such:

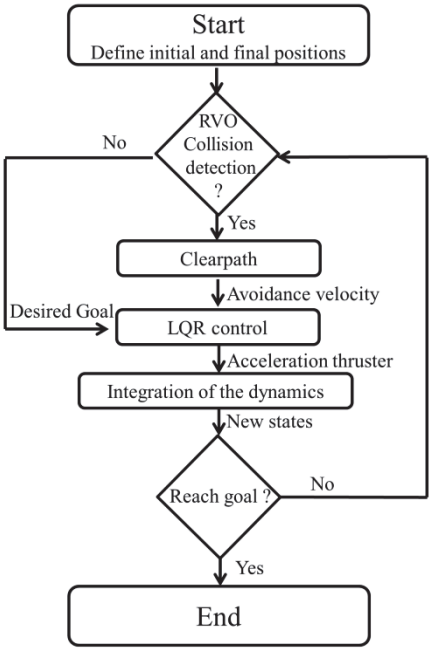

Figure 5. Flow chart of LQR/RVO algorithm.

Algorithm RVO

input : Get position and velocity of each spacecraft

n = number of spacecraft in the environment

For A_i to A_n do

Compute the nearest neighbors (N) of other agents for A_i

For all A_i in N do

Construct velocity obstacle RVO for A_i

Compute preferred velocity for A_i

Select new velocity by using ClearPath and compute new velocity for A_i from RVO that is closest to the preferred velocity.

end for

end for

NUMERICAL SIMULATION AND ANALYSIS

To illustrate the effectiveness and performance of the LQR/RVO algorithm, three scenarios are presented in the next subsections using eccentric reference Earth orbits. In these scenarios, followers are required to change their orbit and then track a predefined target nominal trajectory while collision between the agents of the formation is avoided. For the numerical cases presented in this section, the initial orbital parameters are provided in Table 1. It is assumed that all satellites are spherical with a diameter of 0.5 m (defining the collision distance) and the mass of each spacecraft is 10 kg. Specific impulses (I_{sp}) of thrusters are 300 s. The diagonals of the LQR weight matrixes $\boldsymbol{Q}(t)$ and $\boldsymbol{R}(t)$ are [100 100 100 10 10 10] and [10 10

10] respectively. The performance of the controller is assessed in terms of total maneuver Δv and fuel consumption Δm defined as:

$$\Delta v = \int_{t_0}^{t_f} \|\boldsymbol{u}(t)\| dt \tag{15}$$

and

$$\Delta m = m_0 (1 - \exp(-\Delta v / (I_{sp} g_0)) \tag{16}$$

where Δm and m_0 are total fuel consumption and initial spacecraft mass respectively and g_0 is the gravitational constant on the Earth (9.8 m/s^2).

All simulations run on a PC with an Intel Core i7-6700 at 3.40 GHz with 16 GB of RAM. The numerical integrator used to solve the dynamics is the Runge-Kutta method (ode45) in MATLAB®: RelTol: 1.0×10^{-8} and AbsTol: 1.0×10^{-8}.

Table 1. Initial Keplerian orbital elements for the reference orbit (leader).

Semi-major axis (km)	7,178
Eccentricity	0.02
Inclination (deg)	40
Argument of perigee (deg)	30
Longitude of ascending node (deg)	50
True anomaly (deg)	11

SIMULATION RESULTS

1st SCENARIO

The initial and final satellite and obstacle states are defined in Table 2. Figure 6 shows that the satellite will collide with the obstacle, if no avoidance maneuver is performed. The distance, control inputs of both satellites are shown in Figure 6. The Δv requirement and fuel consumption to avoid collision are shown in Table 2. Due to the collision avoidance maneuver, the fuel consumption increases to 159% with respect to the LQR-only case.

Table 2. Initial relative position of follower and obstacle of the 1st scenario.

Object	Initial position (m)	Initial velocity (m/s)	Final position (m)	Final velocity (m/s)
Satellite	$[0, 20, 10]^T$	$[10, 5, 0]^T$	$[0, 0, 10]^T$	$[0, 0, 0]^T$
Obstacle	$[1.75, 13.71, 6.33]^T$	$[0, 0, 0]^T$	-	-

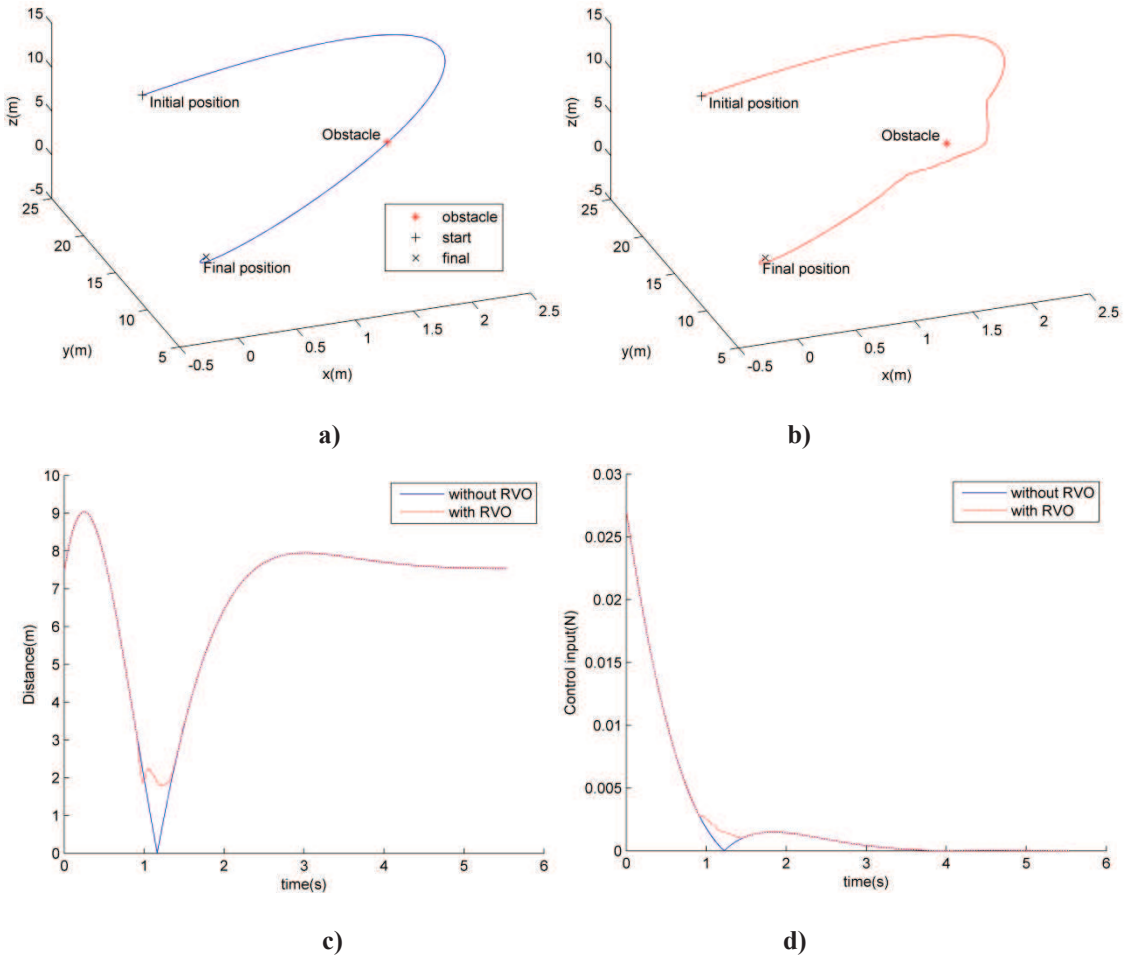

Figure 6. Manoeuver trajectory in the 1st scenario 1 a) without RVO b) with RVO c) distance between the satellite and obstacle d) control input.

Table 3. Summary of the results for the 1st scenario

	Δv (m/s)	Fuel consumption (g)	Maximum control (N)
Without RVO	3.07	10.40	0.27
With RVO	3.15	27.00	0.27

2nd SCENARIO

This scenario simulates the orbit transfer of two satellites with initial and final conditions as indicated in Table 4. In Figure 7, the collision of two satellites is observed during the maneuver without the RVO in the middle of the transfer orbit. This does not occur when the RVO is active. The control inputs and velocities of both satellites are shown in Figure 8. The fuel consumptions of the 1st and 2nd satellites in Table 5 require 6.86% and 11.76% (the difference of the consumption is due to the different initial velocities) more propellant due to the collision avoidance maneuver.

Table 4. Initial relative position of two satellites.

Satellite	Initial position(m)	Initial velocity(m/s)	Final position (m)	Final velocity (m/s)
1	$[0, 20, 10]^T$	$[10, 5, 0]^T$	$[0, 0, 10]^T$	$[0, 0, 0]^T$
2	$[4, 0, 10]^T$	$[-8.4, -7.56, 0]^T$	$[4, 20, 10]^T$	$[0, 0, 0]^T$

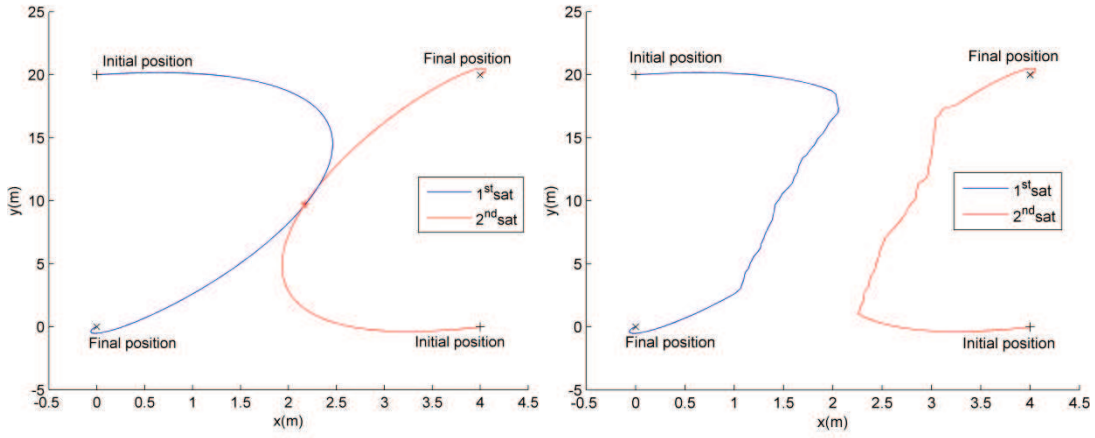

a) **b)**

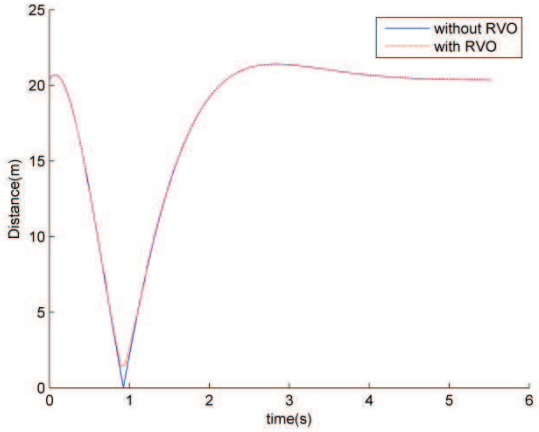

c)

Figure 7. Maneuver trajectory in 2nd scenario a) without RVO b) with RVO c) distance between satellites.

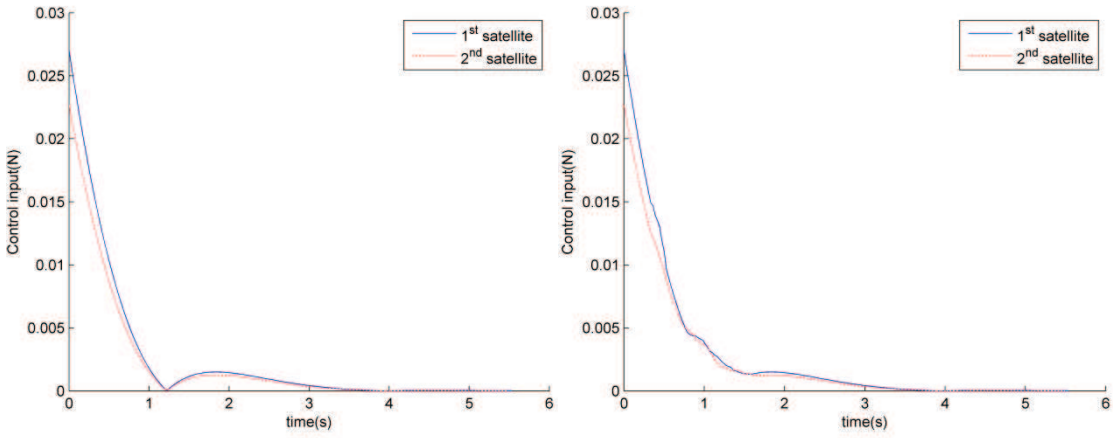

a) **b)**

Figure 8. Control input and velocities with RVO during maneuvering a) 1st satellite b) 2nd satellite.

Table 5. Summary of the results for the 2nd scenario.

	Satellite	Δv (m/s)	Fuel consumption (g)	Maximum control (N)
Without RVO	1	2.99	10.20	0.27
	2	2.51	8.50	0.23
With RVO	1	3.22	10.90	0.27
	2	2.88	9.50	0.23

3rd SCENARIO

In this scenario, four satellites are performing a transfer while avoiding collision among the formation. The objective is to maneuver each satellite to diagonal positions. The initial and final states are defined in Table 6. In the case without RVO in Figure 9(a), the collision is occurred at the origin of LVLH reference frame while including RVO (and other simulation conditions unchanged), any collision is avoided as shown in Figure 9(b). The results of separation distance between each satellite of both without RVO and RVO are provided in Figure 9(c) and (d). The comparison of the 1st satellite trajectory between without RVO and RVO is shown in Figure 10. The thrust behaviors of both cases are observed in Figure 11. Without RVO are required the magnitude trend of control inputs in all satellites because of symmetry of the direction form their initial states to desired goals. In case of with RVO, the magnitude trend of them are required the same values when comparing with. The reason is multi-geometric interpretations of RVO of each are the same pattern. The Δv and fuel consumption for collision avoidance are increased around 2 times as shown in Table 7.

Table 6. Initial and final relative position of two satellites in 3rd scenario.

Satellite	Initial position	Initial velocity (m/s)	Final position (m)	Final velocity (m/s)
1	$[0, -15, 15]^T$	$[0, 0, 0]^T$	$[0, 15, -15]^T$	$[0, 0, 0]^T$
2	$[0, 15, 15]^T$	$[0, 0, 0]^T$	$[0, -15, -15]^T$	$[0, 0, 0]^T$
3	$[0, 15, -15]^T$	$[0, 0, 0]^T$	$[0, -15, 15]^T$	$[0, 0, 0]^T$
4	$[0 -15 -15]^T$	$[0, 0, 0]^T$	$[0, 15, 15]^T$	$[0, 0, 0]^T$

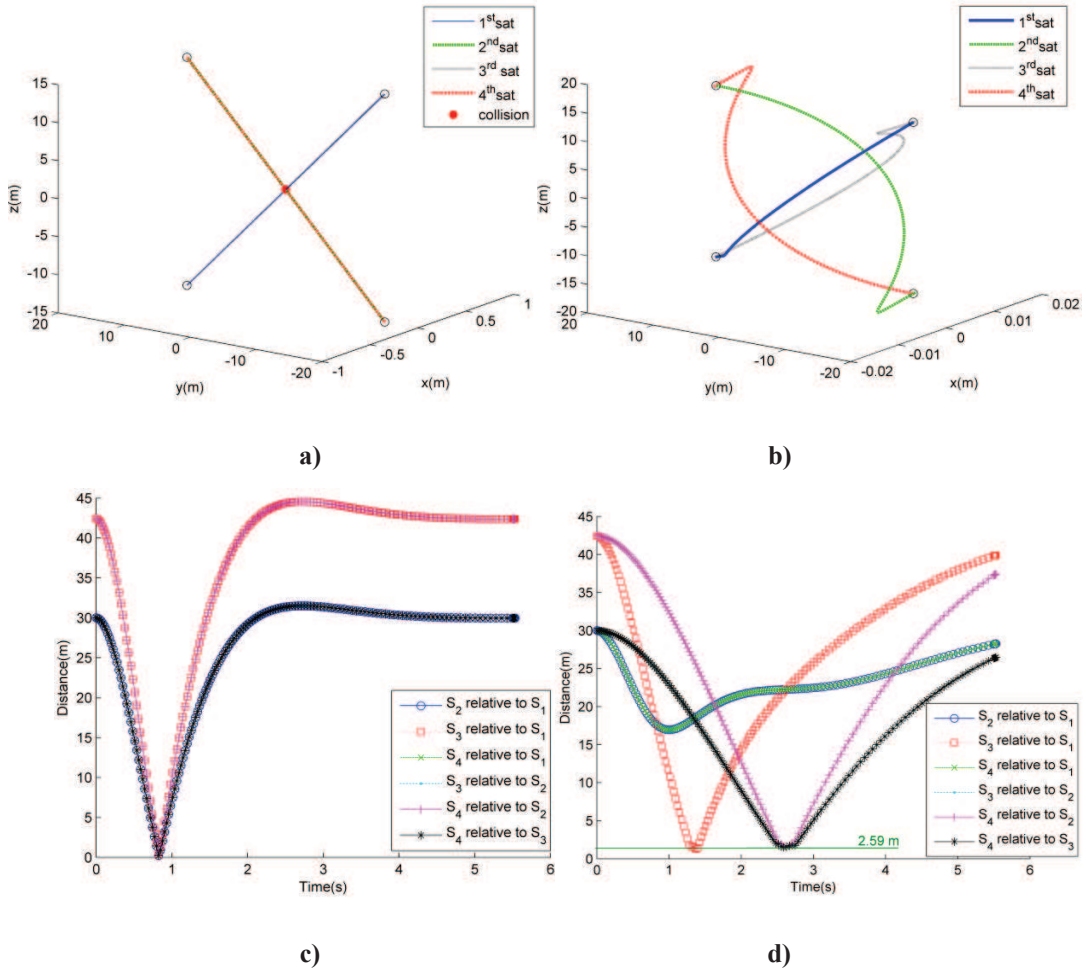

Figure 9. Manoeuver trajectory in 3rd scenario a) without RVO b) with RVO c) distance without RVO d) distance with RVO.

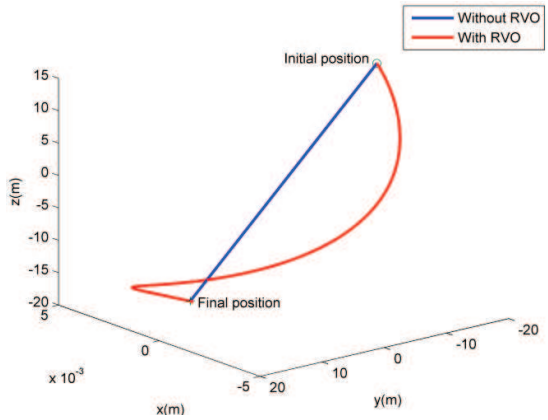

Figure 10. Comparison of the 1st satellite trajectory between without RVO and with RVO.

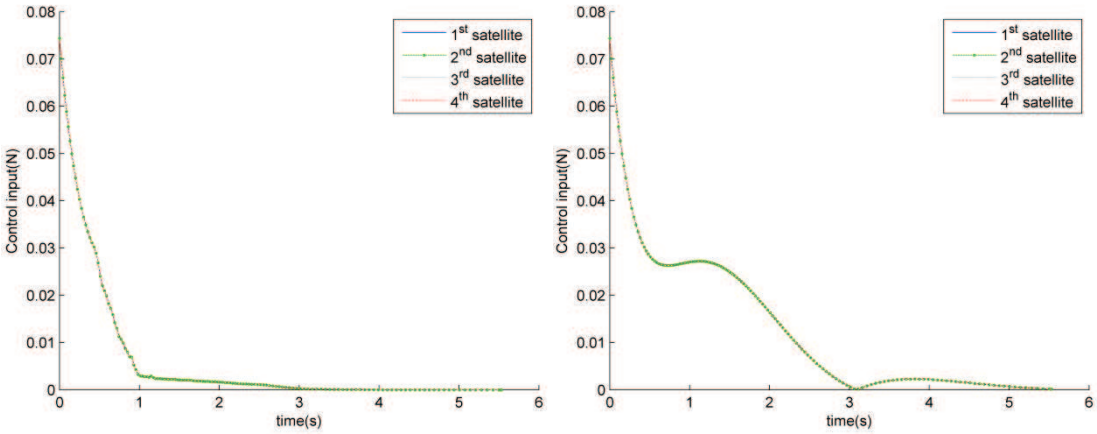

a) **b)**

Figure 11. Control input of the satellites in formation a) without RVO b) with RVO.

Table 7. Summary of the results for the 3rd scenario.

	Satellite	Δv (m/s)	Fuel consumption (g)	Maximum control (N)
Without RVO	1	0.0072	0.184	7.4358e-4
	2	0.0072	0.184	7.4358e-4
	3	0.0072	0.184	7.4358e-4
	4	0.0072	0.184	7.4358e-4
With RVO	1	0.0143	0.365	7.4358e-4
	2	0.0143	0.365	7.4358e-4
	3	0.0143	0.365	7.4358e-4
	4	0.0143	0.365	7.4358e-4

CONCLUSIONS

A distributed LQR/RVO control algorithm for multiple satellites to perform collision avoidance during proximity operations has been presented in this paper. The algorithm was implemented in three scenarios for spacecraft formation. These scenarios show that the controllers have succeeded in creating real-time collision-free and oscillation-free optimum trajectories for all the spacecraft with both static and moving obstacles. However, for effective collision avoidance, the formulation requires that each satellite knows the exact position, velocity, and heading of every other satellite at all times. Then, the constraints of both propulsion and controller are ignored in this paper. Both factors will be considered in the future work.

For future work, we will consider perturbations (J_2 and atmospheric drag) and different reference orbit to test the controller performance and the ability of adaptation according to the dynamical requirements of the problem to improve the collision avoidance system effectiveness and robustness with random initial configurations, measurement uncertainty and the effect of the maximum thrust limitation.

ACKNOWLEDGMENTS

This work was funded by Geo-Informatics and Space Technology Development Agency (public organization).

REFERENCES

[1] Mueller, J. B., Griesemer, P. R., and Thomas, S. J. "Avoidance maneuver planning incorporating station-keeping constraints and automatic relaxation," *Journal of Aerospace Information Systems* Vol. 10, No. 6, 2013.

[2] Schlanbusch, R., Kristiansen, R., and Nicklasson, P. J. "Spacecraft formation reconfiguration with collision avoidance," *Automatica* Vol. 47, 2011, pp. 1443-1449.

[3] Richards, A., Schouwenaars, T., How, J. P., and Feron, E. "Spacecraft Trajectory Planning with Avoidance Constraints Using Mixed-Integer Linear Programming," *Journal of Guidance, Control and Dynamics* Vol. 25, 2002.

[4] Slater, G. L., Byram, S. M., and Williams, T. W. "Collision Avoidance for Satellites in Formation Flight," *Journal of Guidance, Control and Dynamics* Vol. 29, No. 5, 2006.

[5] Wang, S. Q., and Schaub, H. "Spacecraft collision avoidance using coulomb forces with separation distance and rate feedback," *Journal of Guidance Control and Dynamics* Vol. 31, No. 3, 2008, pp. 740-750.

[6] Sauter, L., and Palmer, P. "Onboard semianalytic approach to collision-free formation reconfiguration," *IEEE Transactions on Aerospace and Electronic Systems* Vol. 48, No. 3, 2012.

[7] Zhou, N., and Xia, Y. "Coordination control design for formation reconfiguration of multiple spacecraft," *IET Control Theory & Applications* Vol. 9, No. 15, 2015, pp. 2222-2231.

[8] Palacios, L., Ceriotti, M., and Radice, G. "Close proximity formation flying via linear quadratic tracking controller and artificial ptential funtion," *Advances in Space Research* Vol. 56, 2015, pp. 2167-2176.

[9] Berg, J., Lin, M., and Manocha, D. "Reciprocal Velocity Obstacles for Real-Time Multi-Agent Navigation," *IEEE International Conference on Robots and Automation (ICRA)*. May 2008.

[10] Faverjon, B., and Shiller, Z. "Motion planning in dynamic environments using Velocity Obstacles," *International Journal of Robotics Research* Vol. 17, No. 7, 1998, pp. 760-772.

[11] Allwai, Z. T., and Abdalla, T. Y. "A PSO-Optimized Reciprocal Velocity Obstacles Algorithm for Navigation of Multiple Mobile Robots.," *International Journal of Robotics and Automation (IJRA)* Vol. 4, 2015, pp. 31-40.

[12] Best, A., Narang, S., and Manocha, D. "Real-time Reciprocal Collision Avoidance with Elliptical Agents," *IEEE International Conference on Robotics and Automation (ICRA)*. Stockholm, Sweden, 2016.

[13] Alejo, D., Cobano, J. A., Heredia, G., and Ollero, A. "Optimal Reciprocal Collision Avoidance with Mobile and Static Obstacles for Multi-UAV Systems," *International Conference on Unmanned Aircraft Systems (ICUAS)*. Orlando, FL, 2014.

[14] Snape, J., Guy, S. J., Vembar, D., Lake, A., Lin, M., and Manocha, D. "Reciprocal Collision Avoidance and Navigation for Video Games," *Game Developers Conference (GDC)*. San Francisco, 2012.

[15] Inalhan, G., Tillerson, M., and How, J. P. "Relative Dynamics and Control of Spacecraft Formation in Eccentric Orbits," *Journal of Guidance Control and Dynamics* Vol. 25, No. 61, 2002, pp. 48-59.

[16] Sabatini, M., and Palmerini, G. B. "Linearized Formation-Flying Dynamics in a Perturbed Orbital Environment," *IEEE Aerospace Conference Proceedings*. 2008, pp. 1-13.

[17] Guy, J. S., Chhugani, J., Kim, C., Satish, N., Lin, M., Manocha, D., and Dubey, P. "Clearpath: highly parallel collision avoidance for multi-agent simulation," *ACM SIGGRAPH symposium on computer animation*. New Orleans, Louisiana, 2009, pp. 177-187.